Animal Nutrition 17 (2024) 25–35

Contents lists available at ScienceDirect

Animal Nutrition

journal homepage: http://www.keaipublishing.com/en/journals/aninu/

Original Research Article

Trimethylamine oxide supplementation differentially regulates fat deposition in liver, longissimus dorsi muscle and adipose tissue of growing-finishing pigs

Andong Zha [a, c], Wanquan Li [b], Jing Wang [b], Ping Bai [d], Ming Qi [a, c], Peng Liao [a], Bie Tan [b, *], Yulong Yin [a, b, c, d]

[a] Laboratory of Animal Nutritional Physiology and Metabolic Process, Key Laboratory of Agro-ecological Processes in Subtropical Region, National Engineering Laboratory for Pollution Control and Waste Utilization in Livestock and Poultry Production, Institute of Subtropical Agriculture, Chinese Academy of Sciences, Changsha 410125, China
[b] College of Animal Science and Technology, Hunan Agricultural University, Changsha 410128, China
[c] University of Chinese Academy of Sciences, Beijing 100008, China
[d] Yunnan Southwest Agriculture and Animal Husbandry Group Co., Ltd, Kunming 650224, China

ARTICLE INFO

Article history:
Received 8 March 2023
Received in revised form
22 December 2023
Accepted 29 December 2023
Available online 3 January 2024

Keywords:
Growing-finishing pig
Trimethylamine oxide
Fat deposition
Fatty acid composition
Intestinal microbiota

ABSTRACT

Trimethylamine oxide (TMAO) is a microbiota-derived metabolite, and numerous studies have shown that it could regulate fat metabolism in humans and mice. However, few studies have focused on the effects of TMAO on fat deposition in growing-finishing pigs. This study aimed to investigate the effect of TMAO on fat deposition and intestinal microbiota in growing-finishing pigs. Sixteen growing pigs were randomly divided into 2 groups and fed with a basal diet with 0 or 1 g/kg TMAO for 149 d. The intestinal microbial profiles, fat deposition indexes, and fatty acid profiles were measured. These results showed that TMAO supplementation had a tendency to decrease lean body mass ($P < 0.1$) and significantly increased backfat thickness ($P < 0.05$), but it did not affect growth performance. TMAO significantly increased total protein (TP) concentration, and reduced alkaline phosphatase (ALP) concentration in serum ($P < 0.05$). TMAO increased the α diversity of the ileal microbiota community ($P < 0.05$), and it did not affect the colonic microbial community. TMAO supplementation significantly increased acetate content in the ileum, and *Proteobacteria* and *Escherichia–Shigella* were significantly enriched in the TMAO group ($P < 0.05$). In addition, TMAO decreased fat content, as well as the ratio of linoleic acid, n-6 polyunsaturated fatty acids (PUFA), and PUFA in the liver ($P < 0.05$). On the contrary, TMAO increased intramuscular fat content of the longissimus dorsi muscle, whereas the C18:2n6c ratio was increased, and the n-6 PUFA:PUFA ratio was decreased ($P < 0.05$). In vitro, 1 mM TMAO treatment significantly upregulated the expression of *FASN* and *SREBP1* in C2C12 cells ($P < 0.05$). Nevertheless, TMAO also increased adipocyte area and decreased the *CPT-1B* expression in subcutaneous fat ($P < 0.05$). Taken together, TMAO supplementation regulated ileal microbial composition and acetate production, and regulated fat distribution and fatty acid composition in growing-finishing pigs. These results provide new insights for understanding the role of TMAO in humans and animals.

1. Introduction

Fat deposition is an effective way to store energy in humans and animals, and is closely associated with long-term metabolic health. In growing-finishing pigs, fat deposition is also associated with meat quality. Recent studies have shown that fat deposition is not only associated with genetics, diet and lifestyle, but also significantly associated with gut microbes. Bäckhed et al. (2004) showed that fecal microbiota transplantation regulated fat deposition in

* Corresponding author.
E-mail address: bietan@hunau.edu.cn (B. Tan).
Peer review under responsibility of Chinese Association of Animal Science and Veterinary Medicine.

Production and Hosting by Elsevier on behalf of KeAi

https://doi.org/10.1016/j.aninu.2023.12.006

germ-free mice. In addition, an increasing number of studies also showed that single species also regulate fat deposition. *Akkermansia muciniphila* improves obesity by promoting energy consumption and downregulates perilipin 2 protein expression in mice (Depommier et al., 2020). *Parabacteroides distasonis* increased the circulating succinate and lithocholic acid levels to decrease weight gain and fat storage in mice (Wang et al., 2019a). The colonization of *Prevotella copri* activated chronic inflammatory responses via the TLR4/mTOR pathway and significantly upregulated the expression of lipolysis genes to promote fat deposition in mice (Chen et al., 2021). Therefore, it is an effective way to regulate fat deposition and metabolic homeostasis by intestinal microbiota.

Trimethylamine oxide (TMAO) is an important microbiota-derived metabolite. Red meat and seafood intake is significantly associated with elevated serum TMAO levels (Abbasi, 2019; Hamaya et al., 2020; Wang et al., 2019b). Choline, L-carnitine, and betaine are decomposed into trimethylamine (TMA) by the intestinal microbiota community, and TMA is transformed into TMAO by hepatic flavin-containing monooxygenase 3 (*FMO3*) (Verhaar et al., 2020). The production of TMA depends on the *cutC/cutD/cutA* gene of intestinal microbiota (Rath et al., 2017; Roberts et al., 2018). Clinical trials have shown that cardiovascular disease is associated with high levels of TMAO in the blood (Abbasi, 2019). An increasing number of studies have shown that high levels of TMAO and TMAO precursors (carnitine, choline, betaine) are associated with a higher risk of cardiovascular disease (Fu et al., 2020; Komaroff, 2018; Tang et al., 2019). High levels of circulating TMAO are associated with an increased risk of diabetes and obesity (Dehghan et al., 2020; Zhuang et al., 2019). Trimethylamine oxide induces forkhead box O1 (*Foxo1*) expression by selectively activating the protein kinase R-like endoplasmic reticulum kinase to promote hyperglycemia (Chen et al., 2019). Dietary TMAO supplementation has been found to upregulate the expression of macrophage scavenger receptors (Wang et al., 2011). Long-term TMAO exposure was shown to reduce diet-induced glucose tolerance impairment and reduce adipocyte endoplasmic reticulum stress and lipolysis in mice. In addition, TMAO induces adipogenesis in palmitic acid treated HepG2 cells (Tan et al., 2019). However, limited studies have focused on the effects of TMAO on host fat deposition.

In our study, we performed a TMAO intervention trial in growing-finishing pigs and evaluated the effect of TMAO on fat accumulation, fatty acid composition, and intestinal microbiota.

2. Materials and methods

2.1. Animal ethics statement

The experiment was conducted (No. 20200505) in accordance with the guidelines of the Experimental Animal Ethics Committee of the Institute of Subtropical Agriculture (Changsha, Hunan Province, China). The experiment complied with the ARRIVE guidelines.

2.2. Animal experiment

A total of 16 growing pigs (26.00 ± 2.12 kg) with similar body weight and age were randomly divided into 2 groups ($n = 8$). The NC group were fed a basal diet and the TMAO group were fed the basal diet supplemented with 1 g/kg TMAO (Overland et al., 1999). All pigs had free access to feed and water. Before the experiment, the piggery was disinfected and all pigs were raised in separated pens. The experiment lasted 149 d. Feed intake and body weight were recorded during the experiment. After the experiment, the pigs were fasted for 24 h and weighed to calculate their average daily gain (ADG), average daily feed intake (ADFI), and feed conversion rate. The experiment was conducted in 2020 at the Institute of Subtropical Sciences, Chinese Academy of Sciences.

2.3. Chemical analysis of feed chemical compositions

The basal diet was formulated according to NRC (2012). The ingredients and chemical composition are shown in Table 1. Values of digestible energy were calculated from data provided by Feed Database in China (2020) (Tian et al., 2023). The crude protein (CP) contents in diet were measured using flow injection analysis (AA3, SEAL Analytical Instruments Co., Ltd, Germany) according to the method in DB43/T 2139-2021. The ether extract in diet was measured using a Soxhlet extractor according to method 920.39 (AOAC, 2006; Feng et al., 2023).

2.4. Slaughter experiment

The slaughter experiment was performed according to the China National Standard (Ministry of Agriculture of the People's Republic of China, 2019, 2004). After removing the head, feet, tail and viscera (except kidneys), the carcass was weighed to calculate the slaughter rate. The remainder of the carcass was divided by skin, fat, muscle, and bone, then weighed to calculate lean body percentage, fat percentage, bone percentage, and skin percentage. The thickness of subcutaneous adipose tissue at the 6th to 7th ribs was measured as backfat thickness. In addition, the heart, liver, spleen, lung and kidney were also weighed. Carcass straight length and carcass oblique length were measured according to a previous study (Li et al., 2021b).

2.5. Serum biochemistry index

The serum biochemistry index was measured according to a previous study (Liu et al., 2015; Qi et al., 2022). Blood samples were centrifuged at 835 × *g* for 15 min, and the supernatant was taken for measurement. The serum albumin, total protein (TP),

Table 1
Ingredients and chemical composition of the basal diet (%, as-fed basis).

Ingredients	Content	Chemical composition[2]	Content
Stage 1			
Corn meal	65.00	Digestible energy, MJ/kg	13.90
Soybean meal	25.00	Crude protein	16.75
Wheat bran	6.00	Ether extract	3.08
Premix[1]	4.00		
Stage 2			
Corn meal	65.00	Digestible energy, MJ/kg	13.79
Soybean meal	23.00	Crude protein	17.08
Wheat bran	8.00	Ether extract	2.99
Premix[1]	4.00		
Stage 3			
Corn meal	66.00	Digestible energy, MJ/kg	13.78
Soybean meal	22.00	Crude protein	16.43
Wheat bran	8.00	Ether extract	3.12
Premix[1]	4.00		

[1] Per kilogram of premix contains 405.50 g limestone meal, 270.00 g rice bran, 150.00 g dicalcium phosphate, 80.00 g salt, 32.00 g lysine, 10.00 g choline, 5.20 g phytase, 16.00 g $FeSO_4 \cdot H_2O$, 8.00 g $CuSO_4 \cdot 5H_2O$, 6.00 g $ZnSO_4 \cdot H_2O$, 4.00 g $MnSO_4 \cdot H_2O$, 1.00 g KI, 1.00 g Na_2SeO_3, 3.00 g multienzyme complex, 2.00 g feeding attractant, 1.00 g $CoSO_4 \cdot H_2O$, 1.00 g white sugar, 0.40 g Antioxidant-33 (active compound: ethoxy quinoline), vitamin A 24,375 IU, vitamin B_1 7.5 mg, vitamin B_2 18.75 μg, vitamin B_6 9 mg, vitamin B_{12} 75 mg, vitamin D_3 7,500 IU, vitamin E 60 IU, vitamin K_3 3 7.5 mg, biotin 0.45 mg, folic acid 1.0 mg, D-pantothenic acid 37.5 mg, and nicotinic acid 75 mg.

[2] Values of digestible energy were calculated from data provided by Feed Database in China (2020). Crude protein and ether extracts were measured values.

glutamic-oxaloacetic transaminase, glutamic-pyruvic transaminase, alkaline phosphatase (ALP), urea nitrogen, triglyceride, cholesterol, low-density lipoprotein, high-density lipoprotein, glucose, total bilirubin, creatinine, γ-glutamyl transpeptidase, D-lactate, uric acid, total bile acids, creatine kinase, lipase, complement C3, and complement C4 contents were determined using assay kits (Nanjing Jian Cheng Bioengineering Institute, Jiangsu, China) according to standard operating procedure.

Table 2
Primers used for RT-PCR.

Gene	Primer sequences (5′ to 3′)	Tm, °C
Pig primer		
PPARα	F: CGGGAAAGGCCAGCAAT	60
	R: GGCCACGAGCGTCTTCTC	
Elovl2	F: ATTCTTCACCACCAGCGAGG	60
	R: TGCCTGGCTGTTATCACTCG	
Elovl5	F: TACCACCATGCCACTATGCT	60
	R: GACGTGGATGAAGCTGTTGA	
Elovl6	F: TGAAATTGGGCAAACACTGTGT	60
	R: AGGGCACTTTAAGCACCTCTACA	
Ascl1	F: GAACAGGGTTGCTTTGCTTATT	60
	R: GAGTTCGCCTTTGTTGATGATG	
Scd	F: AAGGAGCTGGTCAGTCGTTG	60
	R: GCTTTCGAAGCTTTGTGCCA	
FADS2	F: ACGGCCTTCATCCTTGCTAC	60
	R: GTTGGCAGAGGCACCCTTTA	
GAPDH	F: ATGGTCCACATGGCCTCCAA	60
	R: GAAGTCAGGAGATGCTCGGTG	
FASD1	F: GTCACTGCCTGGCTCATTCT	60
	R: AGGTGGTTCCACGTAGAGGT	
ACC	F: ATCCCTCCTTGCCTCTCCTA	60
	R: ACTTCCCGTTCAGATTTCCG	
FASN	F: GCCGAGTACAGCGTCAACAACC	60
	R: TGGTCCTTCTTCATCAGCGGGAT	
CPT-1B	F: ACTGTCTGGGCAAACCAAAC	60
	R: CTTCTTGATGAGGCCTTTGC	
LPL	F: CTCGTGCTCAGATGCCCTAC	60
	R: GGCAGGGTGAAAGGGATGTT	
HSL	F: GCAGCATCTTCTTCCGCACA	60
	R: AGCCCTTGCGTAGAGTGACA	
PPARγ	F: TGACCATGGTTGACACCG	60
	R: AAGCATGAACTCCATAGTGG	
FABP4	F: TGGAAACTTGTCTCCAGTG	60
	R: GGTACTTTCTGATCTAATGGTG	
CD36	F: TGTGGATACTTGGAGGTGGG	60
	R: TGCTGGTTGGAATACAGTGG	
ATGL	F: GCGAAAATGTCATCATAACC	60
	R: ATGGTGCTCTTGAGTTCGT	
SREBP1	F: GCACTTTCTGACCCGCTTCTTC	60
	R: CTGCATGGCAACAGGCACCGA	
C2C12 primer		
GAPDH	F: AAGAGGGATGCTGCCCTTAC	60
	R: TACGGCCAAATCCGTTCACA	
SREBP1	F: GCATGCCATGGGCAAGTAC	60
	R: CCACATAGATCTCTGCCAGTGTTG	
PGC1α	F: AACCACACCCACAGGATCAGA	60
	R: TCTTCGCTTTATTGCTCCATGA	
ACC1	F: AAGTCCTTGGTCGGGAAGTATACA	60
	R: ACTCCCTCAAAGTCATCACAAACA	
FASN	F: TGGTGAATTGTCTCCGAAAAGA	60
	R: CACGTTCATCACGAGGTCATG	
PPARγ	F: ATGTCTCACAATGCCATCAGGTT	60
	R: GCTCGCAGATCAGCAGACTCT	

PPARα = peroxisome proliferator activated receptor alpha; *Elovl 2* = ELOVL fatty acid elongase 2; *Elovl 5* = ELOVL fatty acid elongase 5; *Elovl 6* = ELOVL fatty acid elongase 6; *Ascl1* = achaete-scute family bHLH transcription factor 1; *Scd* = stearoyl-CoA desaturase; *FADS2* = fatty acid desaturase 2; *GAPDH* = glyceraldehyde-3-phosphate dehydrogenase; *FADS1* = fatty acid desaturase 1; *Acc* = acetyl-CoA carboxylase; *FASN* = fatty acid synthase; *CPT-1B* = carnitine palmitoyltransferase 1B; *LPL* = lipoprotein lipase; *HSL* = lipase E, hormone sensitive type; *PPARγ* = peroxisome proliferator activated receptor gamma; *FABP4* = fatty acid binding protein 4; *CD36* = CD36 molecule; *ATGL* = patatin-like phospholipase domain containing 2; *SREBP1* = sterol regulatory element binding transcription factor 1; *PGC1α* = PPARG coactivator 1 alpha.

2.6. Hematoxylin and eosin (H&E) staining

H&E staining was performed according to a previous method (He et al., 2022). Longissimus dorsi muscle, liver, and subcutaneous adipose tissue samples were fixed with 4% paraformaldehyde fix solution. Fixed samples were sheared, dehydrated, embedded, sliced, dyed, and sealed in accordance with standard operating procedure. Pathological sections were scanned using a 3D panoramic scanner (PANNORAMIC, 3DHISTECH (Hungary), Japan) (Skydsgaard et al., 2021).

2.7. Medium-long chain fatty acid profiles

The determination of medium-long-chain fatty acid profiles in longissimus dorsi muscle and liver were performed according to previous studies (Bai et al., 2019; Gao et al., 2020; Yin et al., 2017). The fat in the tissue samples was extracted with a mixture solution of benzene and petroleum. Extracted fat was rapidly methylated using 0.4 mol/L sodium hydroxide methanol solution. The supernatant was dried with anhydrous sodium sulfate and then was measured by HPLC (LC1290, Agilent, USA) according to the user's manual.

2.8. Real time fluorescence quantitative PCR

This experiment was conducted according to previous studies (Wang et al., 2016, 2021). The primer sequence is shown in Table 2. The tissue RNA was extracted using the Trizol method. Extracted DNA was tested by 1% agarose gel and a NanoDrop spectrophotometer (Thermo fisher scientific, Waltham, MA, USA) (1.8 < A260:A280 ratio < 2.1). Extracted DNA was reversely transcribed into cDNA by Evo M-MLV assay kits (Accurate Biology, Hunan, China). Then, the cDNA was used as a template to perform a PCR reaction in a fluorescence-based quantitative PCR instrument (Light Cycler 480II, Roche, Switzerland). *GAPDH* was used as the housekeeping gene. Data were analyzed by the $2^{-\Delta\Delta Ct}$ method.

2.9. Determination of short chain fatty acids (SCFAs)

This work was performed according to a previous study (Li et al., 2019). Colonic contents and ileal contents were mixed with

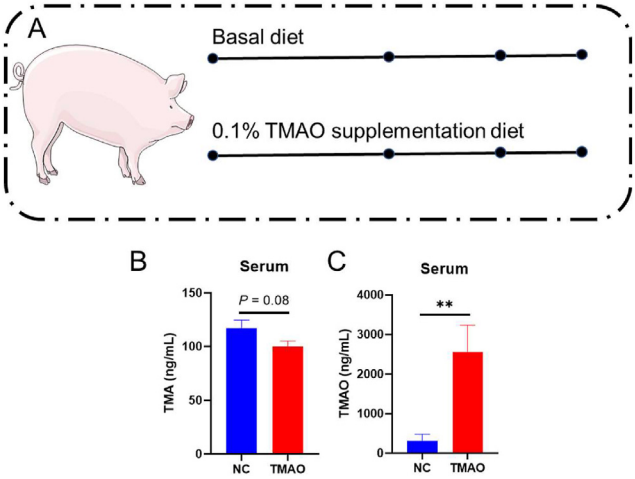

Fig. 1. Experimental design and bar graphs. (A) Experimental design. (B) Serum trimethylamine (TMA) contents. (C) Serum trimethylamine oxide (TMAO) contents. Data are shown as mean ± SEM. $^{**}P < 0.01$. NC group, basal diet; TMAO group, 1 g/kg TMAO supplementation in the basal diet.

Table 3
Effects of trimethylamine oxide (TMAO) on growth performance of finishing pigs.

Item	NC	TMAO	*P*-value
ADG, g/d	572.11 ± 13.264	529.91 ± 29.421	0.21
ADFI, g/d	2108.96 ± 55.636	2060.20 ± 57.525	0.55
Feed conversion rate	3.69 ± 0.044	3.96 ± 0.195	0.21
Lean body mass, kg	49.46 ± 1.594	45.83 ± 1.284	<0.10
Backfat thickness, mm	18.30 ± 0.872[b]	20.89 ± 0.698[a]	0.04
Total protein, g/L	63.75 ± 1.828[b]	69.23 ± 1.726[a]	<0.05

ADFI = average daily food intake, ADG = average daily gain.
NC group, basal diet; TMAO group, 1 g/kg TMAO supplementation in the basal diet. Data are shown as mean ± SEM. Within a row, means without a common superscript differ at $P < 0.05$.

ultrapure water. Then the supernatant was reacted with 25% phosphoric acid solution for 3 h. Then the reaction mixture was tested using LC–MS (7890A, Agilent, USA).

2.10. DNA extraction and 16S rRNA sequencing

This work was conducted in accordance with a previous study (Li et al., 2021a). The bacterial DNA was extracted by the CTAB/SDS method, and assessed by an ultra-micro spectrophotometer (Nanodrop 2000, Thermo Fisher Scientific, USA) and agarose gel electrophoresis. The V3 to V4 region of bacterial 16S rDNA was sequenced by the Illumina Hiseq platform (515F (5′-barcode-GTGCCAGCMGCCGCGG-3′), 907R(5′-CCGTCAATTCMTTTRAGTTT-3′)). The data sequence was analyzed by the Quantitative Insights Into Microbial Ecology (QIIME) pipeline based on operational taxonomic units (OTUs). The sequence data is stored in the SRA database (PRJNA813690).

2.11. Determination of TMAO

This experiment was performed in accordance with a previous study (Jiang et al., 2021). Plasma TMAO was extracted using methanol. The supernatant was measured by UHPLC (1290 Infinity, Agilent, USA) and QTRAP (5500, AB SCIEX, USA).

2.12. Hydrolyzed amino acid profiles

The determination of hydrolyzed amino acid profiles in the longissimus dorsi muscle and liver was performed according to previous protocols (Bai et al., 2019; Long et al., 2016; Yin et al.,

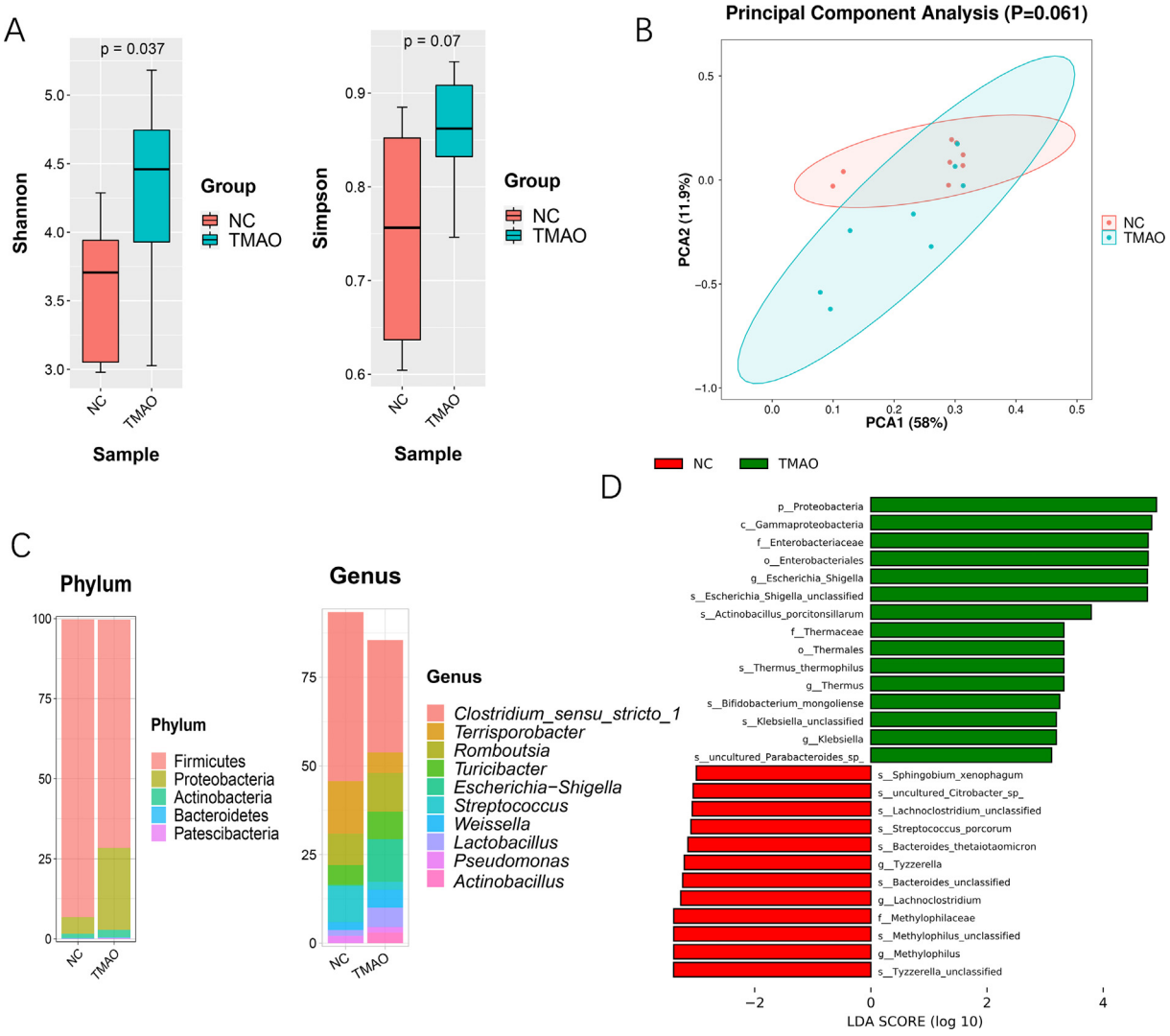

Fig. 2. Trimethylamine oxide (TMAO) regulated ileal microbiota composition. (A) Ileal microbiota α diversity based on Simpson and Shannon indexes. (B) Ileal microbiota β diversity based on principal component analysis (PCA). (C) Ileal microbiota composition at phylum and genus level. (D) LEfSe analysis between NC group and TMAO group. Data are shown as mean ± SEM. NC group, basal diet; TMAO group, 1 g/kg TMAO supplementation in the basal diet.

2017). Tissue samples were hydrolyzed with 6 mol/L hydrochloric acid solution at 110 °C for 22 h. After the filtrate was dried it was dissolved with 0.01 mol/L hydrochloric acid solution. Finally, the solution was tested in an amino acid analyzer (PF8700, Hitachi, Japan).

2.13. C2C12 cell culture

The C2C12 cell was cultured according to a previous study (Zhang et al., 2020). Mouse C2C12 cell line was purchased from American Type Culture Collection and cultured in Dulbecco's modified Eagle's medium containing 10% fetal bovine serum, 50 U/mL penicillin, and 50 μg/mL streptomycin at 37 °C in 5% CO_2 atmosphere. C2C12 cells were seeded in 6 well plates to 70% to 80% confluency. Then, TMAO was added into the cells at a final concentration of 1 mM, 5 mM or 10 mM (Zou et al., 2022), and thereafter the cells were incubated for 48 h.

2.14. Data analysis

Experimental data was sorted by Excel 2019 (Microsoft, Redmond, WA, USA). Data were analyzed by Student's *t*-test using SPSS 22.0 (IBM, Armonk, NY, USA). Data are shown as mean ± SEM, and figures were plotted using Graphpad Prism 8 (La Jolla, CA, USA). The results were considered statistically significant at $P < 0.05$, and $0.05 \leq P < 0.1$ was considered a trend.

3. Results

3.1. TMAO increased fat deposition in growing-finishing pigs

The experimental design is shown in Fig. 1A. Dietary TMAO supplementation significantly increased the serum TMAO concentration ($P < 0.05$), and tended to decrease serum TMA content ($P < 0.1$) (Fig. 1B to C). Dietary TMAO supplementation did not change the ADG, ADFI, and feed conversation rate (Table 3), but tended to decrease the total lean body mass ($P < 0.1$), and increase the backfat thickness ($P < 0.05$) (Table 3). In addition, TMAO supplementation significantly increased serum contents of TP (Table 3).

3.2. TMAO regulated ileal microbiota composition and increased ileal acetate concentration

TMAO is a microbiota-derived metabolite, but there are limited studies focus on its effect on intestinal microbiota composition. Therefore, we performed 16S rDNA sequencing of the ileal and

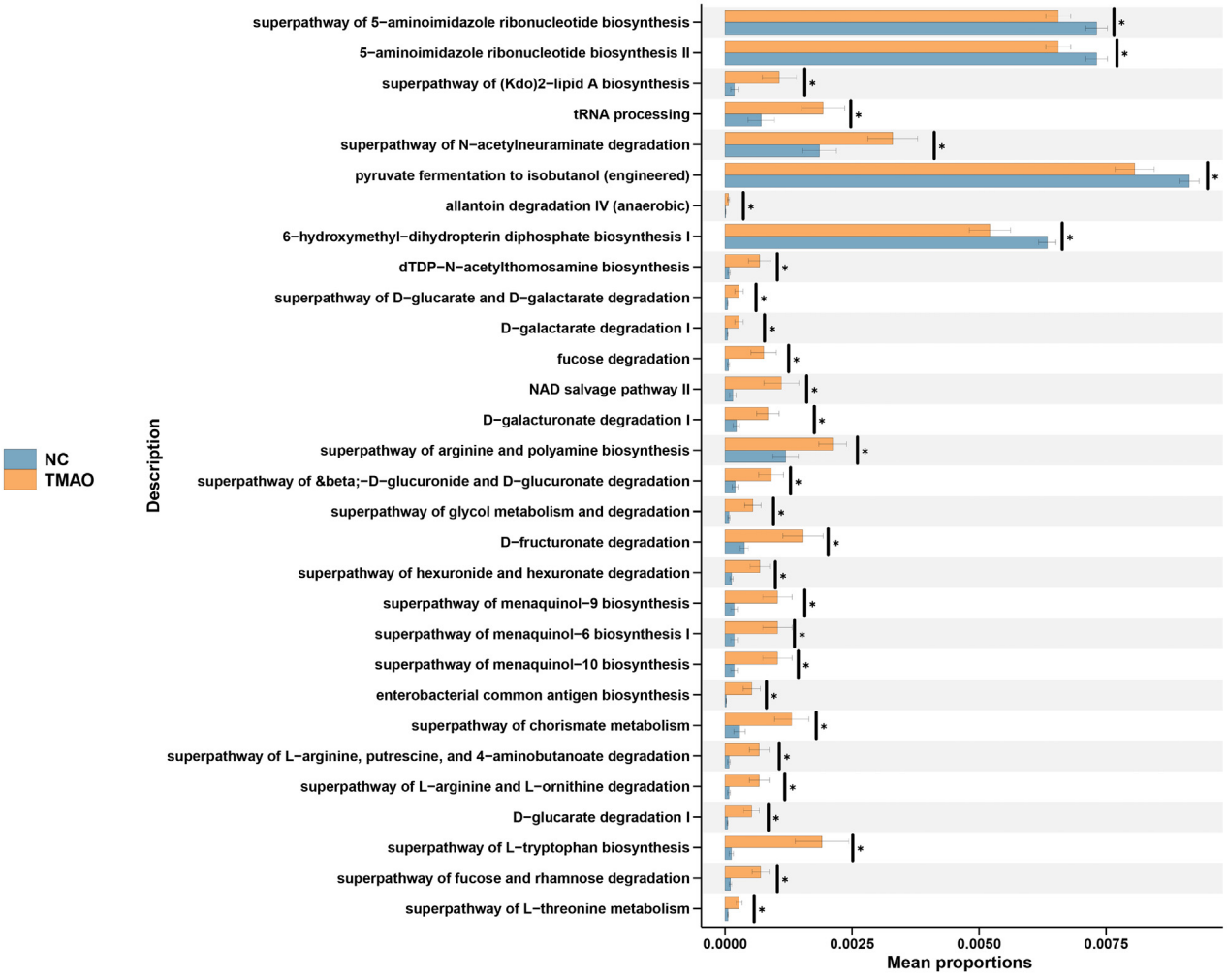

Fig. 3. Trimethylamine oxide (TMAO) regulated ileal microbiota function prediction. NAD = nicotinamide adenine dinucleotide. Data are shown as mean ± SEM. *$P < 0.05$. NC group, basal diet; TMAO group, 1 g/kg TMAO supplementation in the basal diet.

colonic microbiota community. TMAO supplementation significantly increased the richness and evenness of ileal microbiota based on Shannon index ($P < 0.05$), but it did not change the β diversity of ileal microbiota (Fig. 2A to B). The ileal microbial community composition is shown in Fig. 2C. Linear discriminant analysis Effect Size analysis showed that Proteobacteria, and *Escherichia–Shigella* were significantly enriched in the ileal microbiota community of the TMAO group (LDA > 3, Fig. 2D). Moreover, carbohydrate degradation (superpathway of fucose and rhamnose degradation, D-glucarate degradation I, D-fructuronate degradation, D-galacturonate degradation I, fucose degradation, D-galactarate degradation I) was significantly enriched in the TMAO group ($P < 0.05$, Fig. 3). TMAO supplementation did not affect the diversity and richness of the colonic microbiota community (Fig. S1). TMAO had greater effect on the ileal microbial community than the colonic microbial community.

At the phylum level, TMAO increased the relative abundance of Proteobacteria ($P < 0.05$, Fig. 4A). At the genus level, TMAO significantly increased the relative abundance of *Escherichia–Shigella* ($P < 0.05$, Fig. 4B). What is more, TMAO supplementation significantly increased acetate content in the ileum ($P < 0.05$, Fig. 4C). Spearman analysis showed that ileal acetate concentration significantly correlated with the relative abundance of *Escherichia–-Shigella* ($P < 0.05$, Fig. 4D).

3.3. TMAO reduced liver lipid accumulation and regulated fatty acid composition in liver

TMAO supplementation significantly decreased serum ALP levels ($P < 0.05$) (Fig. 5A). Representative H&E staining is shown in Fig. 5B. TMAO significantly decreased liver inflammation and histological score ($P < 0.05$), which indicates TMAO supplementation may contribute to alleviating liver injury (Fig. 5C). TMAO significantly decreased fat content in liver and significantly changed the medium-long chain fatty acid composition ($P < 0.05$, Fig. 5D to E). TMAO also significantly decreased polyunsaturated fatty acids (PUFA) and n-6 PUFA in liver ($P < 0.05$, Fig. 5F). TMAO decreased the relative abundance of C18:2n6c and increased the relative abundance of C20:0 in liver ($P < 0.05$, Fig. 5E). Furthermore, TMAO supplementation significantly decreased P-Ser, and Asp contents in liver ($P < 0.05$, Fig. 5F).

3.4. TMAO increased intramuscular fat content and regulated fatty acid composition in longissimus dorsi muscle

As the H&E staining shows, TMAO did not affect the myofiber area in longissimus dorsi muscle (Fig. 6A to C, $P < 0.05$). TMAO significantly increased intramuscular fat content in longissimus dorsi muscle and it also significantly regulated medium-long chain fatty acid composition ($P < 0.05$, Fig. 6D to E). Specifically, TMAO significantly increased saturated fatty acid (SFA) percentage (C16:0, and C18:0) and n-3 PUFA percentage and decreased n-6 PUFA and unsaturated fatty acid (UFA) percentages in longissimus dorsi muscle ($P < 0.05$, Fig. 6E). TMAO increased C18:2n6C and C20:3n6 percentages in longissimus dorsi muscle ($P < 0.05$, Fig. 6E). TMAO significantly upregulated the mRNA expression of sterol-regulatory element binding protein 1 (*SREBP1*) and downregulated the expression of fatty acid desaturase 2 (*FADS2*) ($P < 0.05$, Fig. 6F). We also investigated the effect of TMAO on fat deposition in C2C12 cells, the 48 h TMAO treatment at 1 mM significantly increased the expression of *SREBP1* and fatty acid synthase (*FASN*) ($P < 0.05$, Fig. 6G).

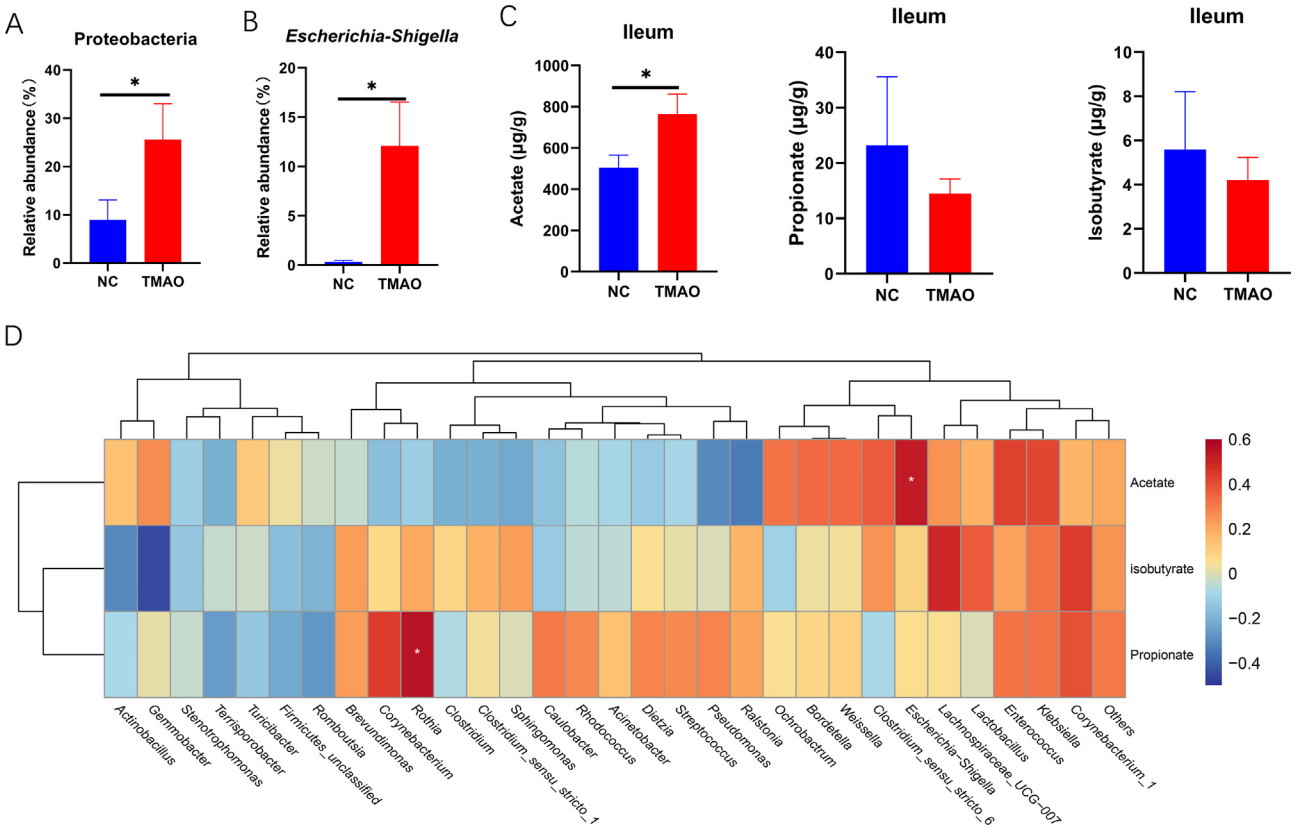

Fig. 4. Trimethylamine oxide (TMAO) regulated ileal acetate concentration in growing-finishing pigs. (A) The relative abundance of Proteobacteria. (B) The relative abundance of *Escherichia–Shigella*. (C) Ileal short chain fatty acid concentration. (D) Spearman analysis between ileal short chain fatty acid concentration and microbiota (genus level). Data are shown as mean ± SEM. *$P < 0.05$. NC group, basal diet; TMAO group, 1 g/kg TMAO supplementation in the basal diet.

3.5. TMAO increased adipocyte area in subcutaneous adipose tissue

Consistent with the previous results, TMAO significantly increased the mean adipocyte area in subcutaneous adipose tissue ($P < 0.05$, Fig. 7A to C), and TMAO supplementation also significantly downregulated the expression of carnitine palmitoyltransferase-1B (*CPT-1B*) ($P < 0.05$, Fig. 7D). TMAO did not affect medium-long chain fatty acid composition.

4. Discussion

Fat deposition is a dynamic equilibrium process of anabolism and catabolism. Fat is synthesized from glycerol and fatty acids. Although most fatty acids come from de novo lipogenesis, fatty acids absorbed from the gut also contribute to fat synthesis in pig (O'hea and Leveille, 1969). In addition, carbohydrates, short-chain fatty acids, and keto acids are also used for lipogenesis and its products are mainly palmitic acid and stearic acid (Nürnberg et al., 1998). Lipogenesis is involved in the cytoplasm and mitochondria. The cytoplasm uses acetyl CoA to produce palmitic acid, while the mitochondria extend palmitic acid and desaturate saturated fatty acids (Ameer et al., 2014). Lipogenesis is modulated by FASN and acetyl-CoA carboxylase lipids are mobilized for energy supply during energy deficit, such as fasting. Lipolysis is mainly carried out in the mitochondria and modulated by HSL, CPT1, LPL, and ATGL enzymes. Fatty acids produced by lipolysis are oxidized in the mitochondria, and CPT1 is a key rate-limiting enzyme in β-oxidation (Morigny et al., 2021).

Accumulated studies have proven that the intestinal microbiota plays an important role in fat deposition and energy homeostasis (Chen et al., 2021; Turnbaugh et al., 2009). Existing literature suggests that TMAO is an important intestinal microbiota-derived metabolite which is closely associated with a series of diseases, such as obesity and metabolic syndrome. *Ihubacter massiliensis* also contributes to TMAO production in animal models (Wu et al., 2020). There are few studies on the effect of TMAO on the intestinal

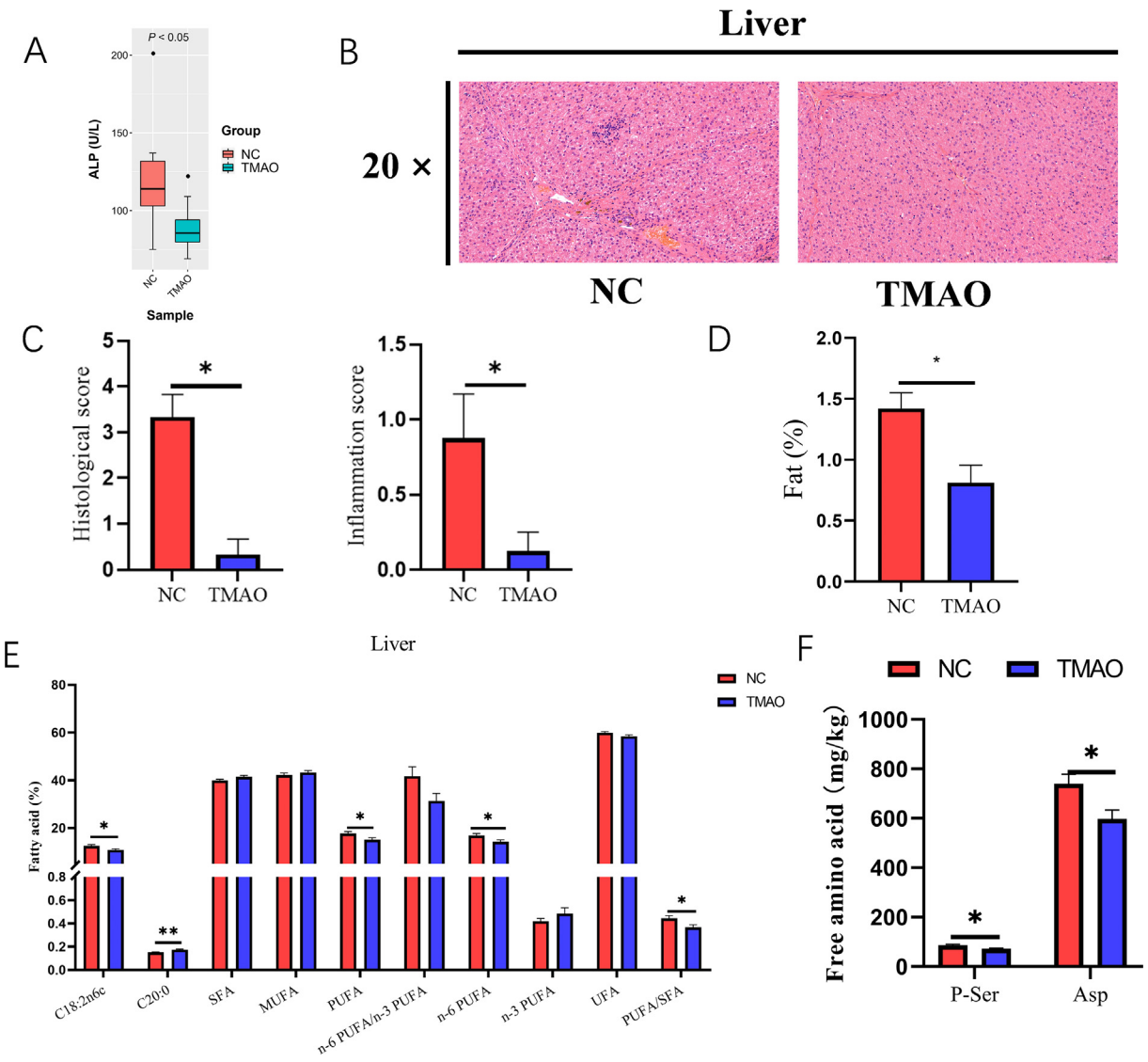

Fig. 5. Trimethylamine oxide (TMAO) reduced inflammation and regulated fat deposition in the liver. (A) Serum alkaline phosphatase (ALP) content. (B) Representative image of hematoxylin and eosin (H&E) staining in liver. (C) Histological and inflammation scores. (D, E, and F) Fat content, fatty acid composition, and free amino acid composition in liver. Data are shown as mean ± SEM. *$P < 0.05$, **$P < 0.01$. NC group, basal diet; TMAO group, 1 g/kg TMAO supplementation in the basal diet. Saturated fatty acid (SFA) = C10:0 + C12:0 + C14:0 + C15:0 + C16:0 + C17:0 + C18:0 + C20:0 + C23:0; monounsaturated fatty acid (MUFA) = C14:1 + C16:1 + C17:1 + C18:1n9t + C18:1n9c + C20:1 + C24:1; polyunsaturated fatty acid (PUFA) = C18:2n6t + C18:2n6c + C18:3n6 + C18:3n3 + C20:3n6 + C20:4n6 + C20:5n3 + C22:6n6; n-3 PUFA = C18:3n3 + C20:5n3; n-6 PUFA = C18:2n6t + C18:2n6c + C18:3n6 + C20:3n6 + C20:4n6 + C22:6n6; UFA = unsaturated fatty acid; Asp = aspartate; P-Ser = phosphoserine.

microbiota and our studies showed that dietary TMAO supplementation increased the richness and diversity of ileal microbiota. TMAO did not affect the α diversity and β diversity of the colonic microbiota. Moreover, TMAO had a limited effect on colonic microbiota function capacity (data not shown). Yoo et al. (2021) reported that a high-fat diet increased circulating TMAO levels by promoting the relative abundance of *Escherichia coli*, and our study also showed that TMAO increased the relative abundance of

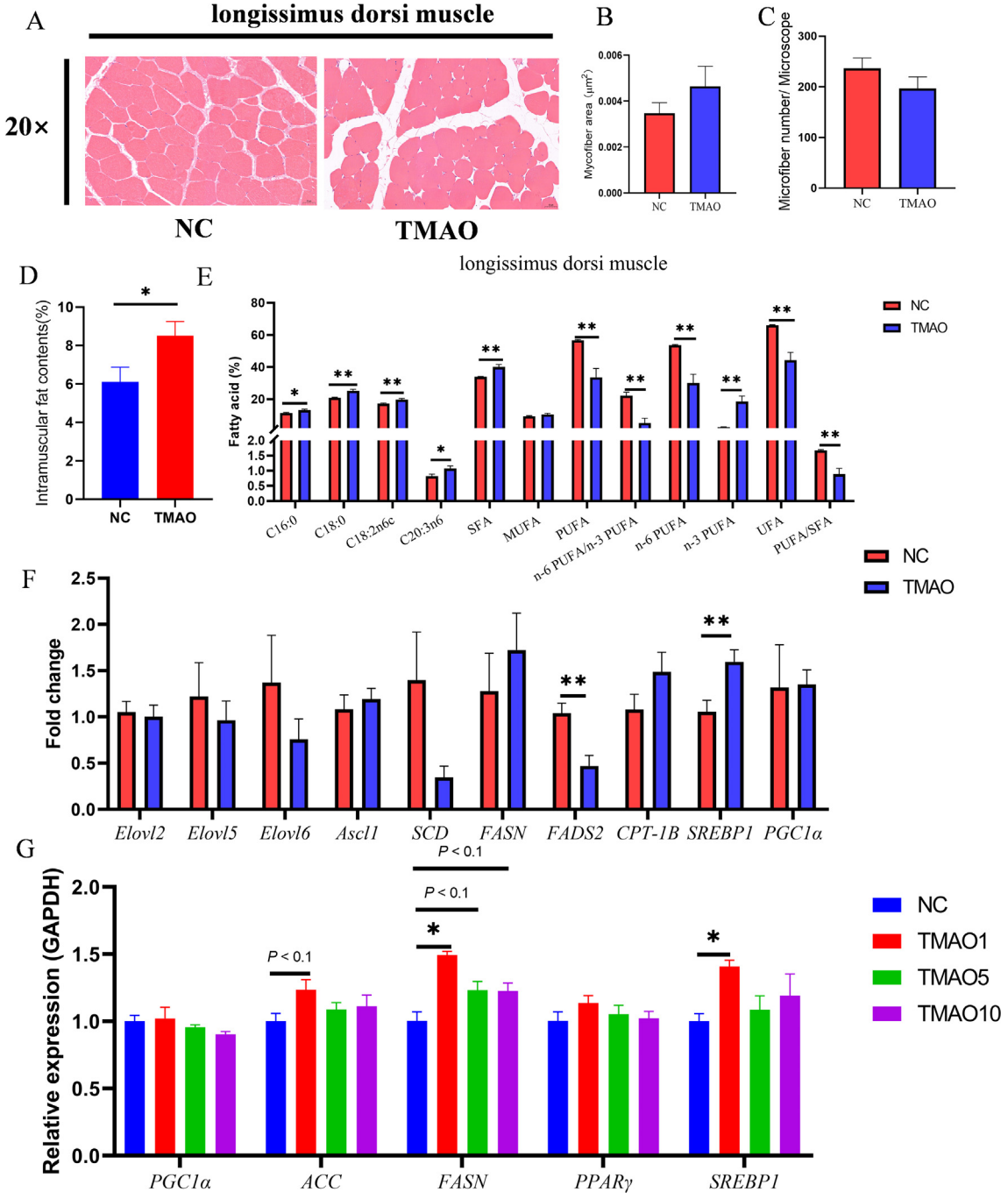

Fig. 6. Trimethylamine oxide (TMAO) increased fat deposition and regulated fatty acid composition. (A) Representative H&E staining image in longissimus dorsi muscle. (B) Myofiber area of longissimus dorsi muscle. (C) Myofiber number/Microscope. (D) Intramuscular fat contents. SFA = C10:0 + C12:0 + C14:0 + C15:0 + C16:0 + C17:0 + C18:0 + C20:0 + C23:0; MUFA = C14:1 + C16:1 + C17:1 + C18:1n9t + C18:1n9c + C20:1 + C24:1; PUFA = C18:2n6t + C18:2n6c + C18:3n6 + C18:3n3 + C20:3n6 + C20:4n6 + C20:5n3 + C22:6n6; n-3 PUFA = C18:3n3 + C20:5n3; n-6 PUFA = C18:2n6t + C18:2n6c + C18:3n6 + C20:3n6 + C20:4n6 + C22:6n6. (E) Fatty acid composition in longissimus dorsi muscle. (F) The mRNA expression in longissimus dorsi muscle. NC group, basal diet; TMAO group, 1 g/kg TMAO supplementation in the basal diet. *Elovl 2* = ELOVL fatty acid elongase 2; *Elovl 5* = ELOVL fatty acid elongase 5; *Elovl 6* = ELOVL fatty acid elongase 6; *Ascl1* = achaete-scute family bHLH transcription factor 1; *SCD* = stearoyl-CoA desaturase; *FADS2* = fatty acid desaturase 2; *FASN* = fatty acid synthase; *CPT-1B* = carnitine palmitoyltransferase 1B; *SREBP1* = sterol regulatory element binding transcription factor 1; *PGC1α* = PPARG coactivator 1 alpha. (G) Effect of TMAO treatment on fat deposition in C2C12 cells (n = 3). *PPARγ* = peroxisome proliferator activated receptor gamma; *SREBP1* = sterol regulatory element binding transcription factor 1; *PGC1α* = PPARG coactivator 1 alpha; *ACC* = acetyl-CoA carboxylase; *FASN* = fatty acid synthase. NC group, 0 mM TMAO treatment; TMAO1 group, 1 mM TMAO treatment; TMAO5 group, 5 mM TMAO treatment; TMAO10 group, 10 mM TMAO treatment. Data are shown as mean ± SEM. $^{*}P < 0.05$, $^{**}P < 0.01$.

Escherichia–Shigella (Yoo et al., 2021). In addition, KEGG analysis showed that carbohydrate degradation was significantly enriched in the TMAO group; these results indicated that TMAO increased the relative abundance of *Escherichia–Shigella* to enhance carbohydrate degradation and acetate production in the ileum. Intragastric administration of acetic acid significantly decreased hepatic lipid accumulation in high-fat-fed mice and upregulated *PPARα*, *UCP2*, and *CPT-1* in HepG2 cells (Kondo et al., 2009). Yamashita et al. (2009) showed that acetate treatment increased the mRNA expression of myoglobin (*Myog*) and *Glut4* in the abdominal muscle. Nevertheless, a previous study also reported that acetate can promote the adipogenic differentiation of IM-BAT cells and significantly upregulates the mRNA expression of *PPARγ* in IM-BAT cells, which also promotes the differentiation of 3T3-L1 cells by upregulating the mRNA expression of *PPARγ2* via activated G-protein coupled receptor 43 (*GPR43*) (Hong et al., 2005; Hu et al., 2016), but this result needs to be demonstrated in vitro.

Alkaline phosphatase (ALP) mainly exists in hepatocytes, and increased serum ALP levels are an important biomarker for acute liver injury. Our study showed that TMAO supplementation decreased serum ALP contents. Further, H&E staining showed that TMAO supplementation significantly decreased the inflammation score and histological score in the liver. Previous studies also showed that injection of TMAO significantly alleviated liver fibrosis in CC_{l4}-challenged mice (Zhou et al., 2022), and oral 120 mg/kg TMAO administration significantly alleviated high-fat high-cholesterol diet-induced steatohepatitis in rats (Zhao et al., 2019). Therefore, we speculated that TMAO has a beneficial effect on liver injury. Moreover, TMAO supplementation decreased the fat content in the liver and this is consistent with a previous study of Zhao et al. (2019). There is also some literature suggesting that TMAO increases fat deposition in the liver (Tan et al., 2019b), however we speculate that this may be due to the dose and animal model being different. In our study, TMAO decreased C18:2n6c (linoleic acid) abundance in the liver. Our study showed that TMAO improved liver injury, decreased fat deposition, and decreased PUFA abundance in the liver. A meta-analysis showed that increased microbiota-derived TMAO increases the risk of obesity (Dehghan et al., 2020). In agreement with a previous study (Dehghan et al., 2020), our results have also shown that TMAO significantly increased backfat thickness in pigs. CPT1 is a key rate-limiting enzyme in β-oxidation, and is located in the mitochondrial outer membrane. It catalyzes the conversion of long chain fatty acids to acetyl-carnitine (Schlaepfer and Joshi, 2020; Yoon et al., 2020). Our results showed that TMAO downregulated the mRNA expression of *CPT-1B* in subcutaneous adipose fat. These results indicated TMAO may inhibit lipolysis to promote fat deposition in subcutaneous adipose tissue in pigs. Intramuscular fat content is an important factor in determining meat quality and our results showed that TMAO significantly increased intramuscular fat content in longissimus dorsi muscle. *SREBP1* is a nuclear transcription factor which is directly involved in fatty acid biosynthesis, triglyceride synthesis, and glucose metabolism (Guo et al., 2014; Hagen et al., 2010). *SREBP1* was significantly upregulated in the TMAO group, indicating that TMAO may upregulated *SREBP1* to increase intramuscular fat content in longissimus dorsi muscle. Mammals do not have Δ 15 desaturase and Δ 12 desaturase and cannot synthesize linoleic acid and linolenic acid. Linoleic acid (C18:2n6c) and linolenic acid (C18:3n3) are essential fatty acids. Our results also showed that TMAO significantly increased the percentages of gamma linoleic acids C18:2n6, C22:3n3, and C20:3n6, and decreased the percentage of C20:4n6 in longissimus dorsi muscle. *FADS2* is a key gene in the polyunsaturated fatty acid anabolism pathway, which can convert linoleic acid and α-linolenic acid into γ-linolenic acid and stearidonic acid (Glaser et al., 2010; Zhang et al., 2016). The mRNA expression of *FADS2* was significantly downregulated in the TMAO group, indicating that TMAO increased the percentage of C18:2n6 via *FADS2* in longissimus dorsi muscle, however these results need to be further verified in vitro.

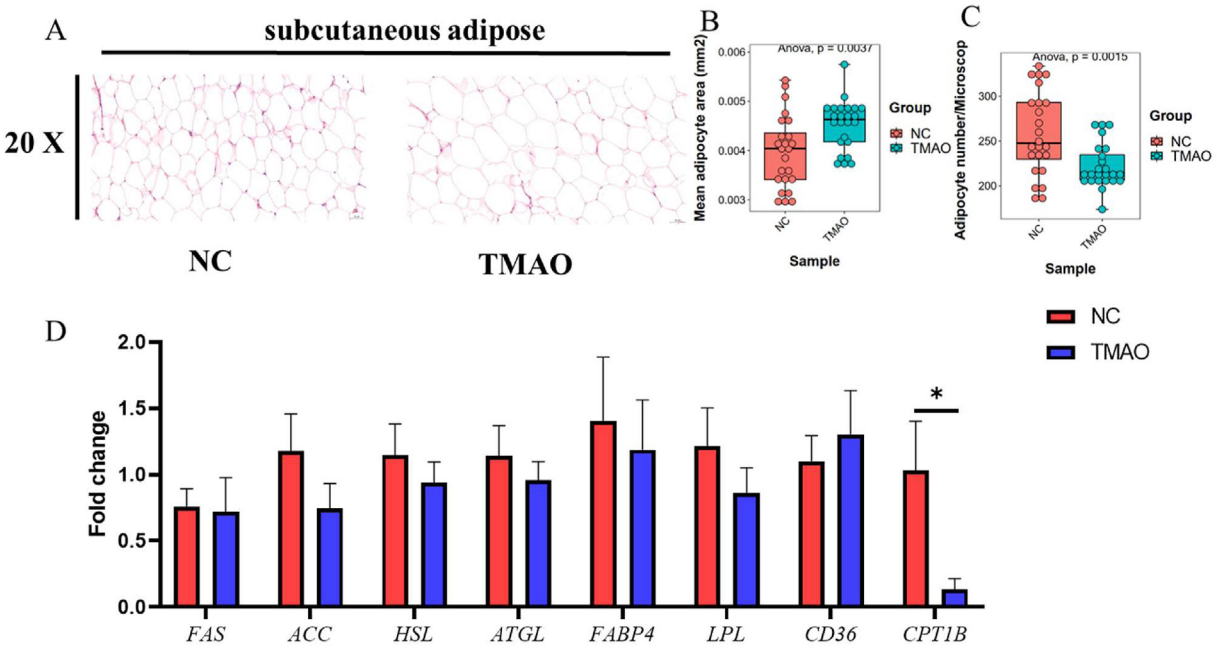

Fig. 7. Trimethylamine oxide (TMAO) decreased lipolysis in subcutaneous adipose tissue. (A) H&E stained image. (B) Mean adipocyte area. (C) Adipocyte number. (D) The mRNA expression in subcutaneous adipose tissue. *FAS* = fatty acid synthase; *ACC* = acetyl-CoA carboxylase; *HSL* = lipase E, hormone sensitive type; *ATGL* = patatin-like phospholipase domain containing 2; *FABP4* = fatty acid binding protein 4; *LPL* = lipoprotein lipase; *CD36* = CD36 molecule; *CPT-1B* = carnitine palmitoyltransferase 1B; *GAPDH* = glyceraldehyde-3-phosphate dehydrogenase. Data are shown as mean ± SEM. *$P < 0.05$. NC group, basal diet; TMAO group, 1 g/kg TMAO supplementation in the basal diet.

5. Conclusion

Taken together, our study demonstrated that TMAO modulated ileal microbiota composition and increased ileal acetate concentration by increasing the relative abundance of *Escherichia–Shigella*. TMAO also regulated fat distribution in different tissues, which increased fat deposition in longissimus dorsi muscle and subcutaneous adipose tissue, and decreased fat deposition in the liver. In addition, TMAO also decreased the percentage of C18:2n6c in the liver, and increased the percentage of C18:2n6c in longissimus dorsi muscle. In conclusion, our results indicated that dietary TMAO supplementation significantly regulated fat distribution in pigs.

Author contributions

Andong Zha and **Wanquan Li:** Writing–Original draft preparation, Conducting the research; **Jing Wang** and **Ming Qi:** Investigation; **Ping Bai, Peng Liao, Bie Tan** and **Yulong Yin:** Research design, Funding acquisition.

Declaration of competing interest

We declare that we have no financial and personal relationships with other people or organizations that can inappropriately influence our work, and there is no professional or other personal interest of any nature or kind in any product, service and/or company that could be construed as influencing the content of this paper.

Acknowledgments

This research was supported by the National Natural Science Foundation of China (U20A2054), the earmarked fund for China Agriculture Research System (CARS-35), and the Science and Technology Major Project of Yunnan Province (202202AE090032), and Large-scale Healthy Breeding Technology Research and Industrialization Demonstration of pig (202102AE090046).

Appendix supplementary data

Supplementary data to this article can be found online at https://doi.org/10.1016/j.aninu.2023.12.006.

References

Abbasi J. TMAO and heart disease: the new red meat risk? JAMA 2019;321:2149–51.
Ameer F, Scandiuzzi L, Hasnain S, Kalbacher H, Zaidi N. De novo lipogenesis in health and disease. Metabolism 2014;63:895–902.
AOAC. Official Methods of Analysis. 18th ed. Gaithersburg, MD: AOAC International; 2006.
Bäckhed F, Ding H, Wang T, Hooper LV, Koh GY, Nagy A, Semenkovich CF, Gordon JI. The gut microbiota as an environmental factor that regulates fat storage. Proc Natl Acad Sci U S A 2004;101:15718–23.
Bai M, Liu H, Xu K, Zhang X, Deng B, Tan C, Deng J, Bing P, Yin Y. Compensation effects of coated cysteamine on meat quality, amino acid composition, fatty acid composition, mineral content in dorsal muscle and serum biochemical indices in finishing pigs offered reduced trace minerals diet. Sci China Life Sci 2019;62:1550–3.
Chen C, Fang S, Wei H, He M, Fu H, Xiong X, Zhou Y, Wu J, Gao J, Yang H, Huang L. Prevotella copri increases fat accumulation in pigs fed with formula diets. Microbiome 2021;9:175.
Chen S, Henderson A, Petriello MC, Romano KA, Gearing M, Miao J, Schell M, Sandoval-Espinola WJ, Tao J, Sha B, Graham M, Crooke R, Kleinridders A, Balskus EP, Rey FE, Morris AJ, Biddinger SB. Trimethylamine n-oxide binds and activates perk to promote metabolic dysfunction. Cell Metabol 2019;30:1141–1151.e5.
Dehghan P, Farhangi MA, Nikniaz L, Nikniaz Z, Asghari-Jafarabadi M. Gut microbiota-derived metabolite trimethylamine n-oxide (TMAO) potentially increases the risk of obesity in adults: an exploratory systematic review and dose-response meta- analysis. Obes Rev 2020;21:e12993.
Depommier C, Van Hul M, Everard A, Delzenne NM, De Vos WM, Cani PD. Pasteurized akkermansia muciniphila increases whole-body energy expenditure and fecal energy excretion in diet-induced obese mice. Gut Microbes 2020;11:1231–45.
Feed Database in China. Tables of feed composition and nutritive values in China. 2020 [in Chinese], https://www.chinafeeddata.org.cn/admin/Login/slcfb. [Accessed 31 December 2020].
Feng G, Li R, Jiang X, Yang G, Tian M, Xiang Q, et al. Prediction of available energy and amino acid digestibility of Chinese sorghum fed to growing-finishing pigs. J Anim Sci 2023;101:skad262.
Fu BC, Hullar MAJ, Randolph TW, Franke AA, Monroe KR, Cheng I, Wilkens LR, Shepherd JA, Madeleine MM, Le Marchand L, Lim U, Lampe JW. Associations of plasma trimethylamine n-oxide, choline, carnitine, and betaine with inflammatory and cardiometabolic risk biomarkers and the fecal microbiome in the multiethnic cohort adiposity phenotype study. Am J Clin Nutr 2020;111:1226–34.
Gao LM, Liu YL, Zhou X, Zhang Y, Wu X, Yin YL. Maternal supplementation with uridine influences fatty acid and amino acid constituents of offspring in a sow-piglet model. Br J Nutr 2020:1–14.
Glaser C, Heinrich J, Koletzko B. Role of FADS1 and FADS2 polymorphisms in polyunsaturated fatty acid metabolism. Metabolism 2010;59:993–9.
Guo D, Bell EH, Mischel P, Chakravarti A. Targeting SREBP-1-driven lipid metabolism to treat cancer. Curr Pharm Des 2014;20:2619–26.
Hagen RM, Rodriguez-Cuenca S, Vidal-Puig A. An allostatic control of membrane lipid composition by SREBP1. FEBS Lett 2010;584:2689–98.
Hamaya R, Ivey KL, Lee DH, Wang M, Li J, Franke A, Sun Q, Rimm EB. Association of diet with circulating trimethylamine-n-oxide concentration. Am J Clin Nutr 2020;112:1448–55.
He L, Zhou X, Liu Y, Zhou L, Li F. Fecal mir-142a-3p from dextran sulfate sodium-challenge recovered mice prevents colitis by promoting the growth of *Lactobacillus reuteri*. Mol Ther 2022;30:388–99.
Hong YH, Nishimura Y, Hishikawa D, Tsuzuki H, Miyahara H, Gotoh C, Choi KC, Feng DD, Chen C, Lee HG, Katoh K, Roh SG, Sasaki S. Acetate and propionate short chain fatty acids stimulate adipogenesis via GPCR43. Endocrinology 2005;146:5092–9.
Hu J, Kyrou I, Tan BK, Dimitriadis GK, Ramanjaneya M, Tripathi G, Patel V, James S, Kawan M, Chen J, Randeva HS. Short-chain fatty acid acetate stimulates adipogenesis and mitochondrial biogenesis via GPR43 in brown adipocytes. Endocrinology 2016;157:1881–94.
Jiang S, Shui Y, Cui Y, Tang C, Wang X, Qiu X, Hu W, Fei L, Li Y, Zhang S, Zhao L, Xu N, Dong F, Ren X, Liu R, Persson PB, Patzak A, Lai EY, Wei Q, Zheng Z. Gut microbiota dependent trimethylamine n-oxide aggravates angiotensin ii-induced hypertension. Redox Biol 2021;46:102115.
Komaroff AL. The microbiome and risk for atherosclerosis. JAMA 2018;319:2381–2.
Kondo T, Kishi M, Fushimi T, Kaga T. Acetic acid upregulates the expression of genes for fatty acid oxidation enzymes in liver to suppress body fat accumulation. J Agric Food Chem 2009;57:5982–6.
Li H, Li H, Xie P, Li Z, Yin Y, Blachier F, Kong X. Dietary supplementation with fermented mao-tai lees beneficially affects gut microbiota structure and function in pigs. Amb Express 2019;9:26.
Li H, Ma L, Li Z, Yin J, Tan B, Chen J, Jiang Q, Ma X. Evolution of the gut microbiota and its fermentation characteristics of ningxiang pigs at the young stage. Animals 2021a;11:638.
Li LY, Xiao SJ, Tu JM, Zhang ZK, Zheng H, Huang LB, Huang ZY, Yan M, Liu XD, Guo YM. A further survey of the quantitative trait loci affecting swine body size and carcass traits in five related pig populations. Anim Genet 2021b;52:621–32.
Liu Y, Kong X, Jiang G, Tan B, Deng J, Yang X, Li F, Xiong X, Yin Y. Effects of dietary protein/energy ratio on growth performance, carcass trait, meat quality, and plasma metabolites in pigs of different genotypes. J Anim Sci Biotechnol 2015;6:36.
Long C, Zhou X, Wang Q, Xie C, Li F, Fan Z, Zhang B, Ruan Z, Chen X, Wu X, Yin Y. Dietary supplementation of lonicera macranthoides leaf powder improves amino acid profiles in serum and longissimus thoracis muscle of growing-finishing pigs. Anim Nutr 2016;2:271–5.
Ministry of Agriculture of the People's Republic of China. Technical regulation for testing of carcass traits in lean-type pig (NY/T 825-2004). Beijing, China: China Agriculture Press; 2004.
Ministry of Agriculture of the People's Republic of China. Technical code of practice for pork quality assessement (NY/T 821-2019). Beijing, China: China Agriculture Press; 2019.
Morigny P, Boucher J, Arner P, Langin D. Lipid and glucose metabolism in white adipocytes: pathways, dysfunction and therapeutics. Nat Rev Endocrinol 2021;17:276–95.
Nürnberg K, Wegner J, Ender K. Factors influencing fat composition in muscle and adipose tissue of farm animals. Livest Prod Sci 1998;56:145–56.
NRC (National Research Council). Nutrient requirements of swine. 11th ed. Washington (DC): National Academy Press; 2012.
O'hea EK, Leveille GA. Significance of adipose tissue and liver as sites of fatty acid synthesis in the pig and the efficiency of utilization of various substrates for lipogenesis. J Nutr 1969;99:338–44.
Overland M, Rørvik KA, Skrede A. Effect of trimethylamine oxide and betaine in swine diets on growth performance, carcass characteristics, nutrient digestibility, and sensory quality of pork. J Anim Sci 1999;77:2143–53.
Qi M, Wang N, Xiao Y, Deng Y, Zha A, Tan B, Wang J, Yin Y, Liao P. Ellagic acid ameliorates paraquat-induced liver injury associated with improved gut microbial profile. Environ Pollut 2022;293:118572.

Rath S, Heidrich B, Pieper DH, Vital M. Uncovering the trimethylamine-producing bacteria of the human gut microbiota. Microbiome 2017;5:54.
Roberts AB, Gu X, Buffa JA, Hurd AG, Wang Z, Zhu W, Gupta N, Skye SM, Cody DB, Levison BS, Barrington WT, Russell MW, Reed JM, Duzan A, Lang JM, Fu X, Li L, Myers AJ, Rachakonda S, Didonato JA, Brown JM, Gogonea V, Lusis AJ, Garcia-Garcia JC, Hazen SL. Development of a gut microbe–targeted nonlethal therapeutic to inhibit thrombosis potential. Nat Med 2018;24:1407–17.
Schlaepfer IR, Joshi M. CPT1A-mediated fat oxidation, mechanisms, and therapeutic potential. Endocrinology 2020;161:bqz046.
Skydsgaard M, Dincer Z, Haschek WM, Helke K, Jacob B, Jacobsen B, Jeppesen G, Kato A, Kawaguchi H, Mckeag S, Nelson K, Rittinghausen S, Schaudien D, Vemireddi V, Wojcinski ZW. International harmonization of nomenclature and diagnostic criteria (inhand): nonproliferative and proliferative lesions of the minipig. Toxicol Pathol 2021;49:110–228.
Tan X, Liu Y, Long J, Chen S, Liao G, Wu S, Li C, Wang L, Ling W, Zhu H. Trimethylamine n-oxide aggravates liver steatosis through modulation of bile acid metabolism and inhibition of farnesoid x receptor signaling in nonalcoholic fatty liver disease. Mol Nutr Food Res 2019;63:e1900257.
Tang WHW, Li DY, Hazen SL. Dietary metabolism, the gut microbiome, and heart failure. Nat Rev Cardiol 2019;16:137–54.
Tian J, Yang F, Bao X, Jiang Q, Li Y, Yao K, et al. Dietary alpha-ketoglutarate supplementation improves bone growth, phosphorus digestion, and growth performance in piglets. Animals 2023;13:569.
Turnbaugh PJ, Hamady M, Yatsunenko T, Cantarel BL, Duncan A, Ley RE, Sogin ML, Jones WJ, Roe BA, Affourtit JP, Egholm M, Henrissat B, Heath AC, Knight R, Gordon JI. A core gut microbiome in obese and lean twins. Nature 2009;457:480–4.
Verhaar BJH, Prodan A, Nieuwdorp M, Muller M. Gut microbiota in hypertension and atherosclerosis: a review. Nutrients 2020;12:2982.
Wang J, Xiao Y, Li J, Qi M, Tan B. Serum biochemical parameters and amino acids metabolism are altered in piglets by early-weaning and proline and putrescine supplementations. Anim Nutr 2021;7:334–45.
Wang J, Zeng L, Tan B, Li G, Huang B, Xiong X, Li F, Kong X, Liu G, Yin Y. Developmental changes in intercellular junctions and kv channels in the intestine of piglets during the suckling and post-weaning periods. J Anim Sci Biotechnol 2016;7:4.
Wang K, Liao M, Zhou N, Bao L, Ma K, Zheng Z, Wang Y, Liu C, Wang W, Wang J, Liu S-J, Liu H. Parabacteroides distasonis alleviates obesity and metabolic dysfunctions via production of succinate and secondary bile acids. Cell Rep 2019a;26:222–235.e5.
Wang Z, Bergeron N, Levison BS, Li XS, Chiu S, Jia X, Koeth RA, Li L, Wu Y, Tang WHW, Krauss RM, Hazen SL. Impact of chronic dietary red meat, white meat, or non-meat protein on trimethylamine n-oxide metabolism and renal excretion in healthy men and women. Eur Heart J 2019b;40:583–94.
Wang Z, Klipfell E, Bennett BJ, Koeth R, Levison BS, Dugar B, Feldstein AE, Britt EB, Fu X, Chung YM, Wu Y, Schauer P, Smith JD, Allayee H, Tang WH, Didonato JA, Lusis AJ, Hazen SL. Gut flora metabolism of phosphatidylcholine promotes cardiovascular disease. Nature 2011;472:57–63.
Wu W-K, Panyod S, Liu P-Y, Chen C-C, Kao H-L, Chuang H-L, Chen Y-H, Zou H-B, Kuo H-C, Kuo C-H, Liao B-Y, Chiu THT, Chung C-H, Lin AY-C, Lee Y-C, Tang S-L, Wang J-T, Wu Y-W, Hsu C-C, Sheen L-Y, Orekhov AN, Wu M-S. Characterization of TMAO productivity from carnitine challenge facilitates personalized nutrition and microbiome signatures discovery. Microbiome 2020;8:162.
Yamashita H, Maruta H, Jozuka M, Kimura R, Iwabuchi H, Yamato M, Saito T, Fujisawa K, Takahashi Y, Kimoto M, Hiemori M, Tsuji H. Effects of acetate on lipid metabolism in muscles and adipose tissues of type 2 diabetic otsuka long-evans tokushima fatty (OLETF) rats. Biosci Biotechnol Biochem 2009;73:570–6.
Yin J, Li Y, Zhu X, Han H, Ren W, Chen S, Bin P, Liu G, Huang X, Fang R, Wang B, Wang K, Sun L, Li T, Yin Y. Effects of long-term protein restriction on meat quality, muscle amino acids, and amino acid transporters in pigs. J Agric Food Chem 2017;65:9297–304.
Yoo W, Zieba JK, Foegeding NJ, Torres TP, Shelton CD, Shealy NG, Byndloss AJ, Cevallos SA, Gertz E, Tiffany CR, Thomas JD, Litvak Y, Nguyen H, Olsan EE, Bennett BJ, Rathmell JC, Major AS, Bäumler AJ, Byndloss MX. High-fat diet induced colonocyte dysfunction escalates microbiota-derived trimethylamine-n-oxide. Science 2021;373:813–8.
Yoon H, Spinelli JB, Zaganjor E, Wong SJ, German NJ, Randall EC, Dean A, Clermont A, Paulo JA, Garcia D, Li H, Rombold O, Agar NYR, Goodyear LJ, Shaw RJ, Gygi SP, Auwerx J, Haigis MC. PHD3 loss promotes exercise capacity and fat oxidation in skeletal muscle. Cell Metab 2020;32:215–228.e7.
Zhang JY, Kothapalli KS, Brenna JT. Desaturase and elongase-limiting endogenous long-chain polyunsaturated fatty acid biosynthesis. Curr Opin Clin Nutr Metab Care 2016;19:103–10.
Zhang L, Duan Y, Guo Q, Wang W, Li F. A selectively suppressing amino acid transporter: sodium-coupled neutral amino acid transporter 2 inhibits cell growth and mammalian target of rapamycin complex 1 pathway in skeletal muscle cells. Anim Nutr 2020;6:513–20.
Zhao ZH, Xin FZ, Zhou D, Xue YQ, Liu XL, Yang RX, Pan Q, Fan JG. Trimethylamine n-oxide attenuates high-fat high-cholesterol diet-induced steatohepatitis by reducing hepatic cholesterol overload in rats. World J Gastroenterol 2019;25:2450–62.
Zhou D, Zhang J, Xiao C, Mo C, Ding BS. Trimethylamine-n-oxide (TMAO) mediates the crosstalk between the gut microbiota and hepatic vascular niche to alleviate liver fibrosis in nonalcoholic steatohepatitis. Front Immunol 2022;13:964477.
Zhuang R, Ge X, Han L, Yu P, Gong X, Meng Q, Zhang Y, Fan H, Zheng L, Liu Z, Zhou X. Gut microbe-generated metabolite trimethylamine n-oxide and the risk of diabetes: a systematic review and dose-response meta-analysis. Obes Rev 2019;20:883–94.
Zou H, Huang C, Zhou L, Lu R, Zhang Y, Lin D. NMR-based metabolomic analysis for the effects of trimethylamine n-oxide treatment on C2c12 myoblasts under oxidative stress. Biomolecules 2022;12:1288.